Response to Comment on "Vapor Lubrication for Reducing Water and Ice Adhesion on Poly(dimethylsiloxane) Brushes": Organic Vapors Influence Water Contact Angles on Hydrophobic Surfaces

Shuai Li and Hans-Jürgen Butt*

Fast removal of water drops from solid surfaces is important in many applications such as on solar panels in rain, in heat transfer, and for water collection. Recently, a reduction in lateral adhesion of water drops on poly(dimethylsiloxane) (PDMS) brush surfaces after exposure to various organic vapors was reported. It was attributed to the physisorption of vapor and swelling of the PDMS brushes. However, it was later pointed out that a change in the interfacial energies by vapor adsorption could also have caused low drop adhesion. To find out how strongly each effect contributes, contact angles of water drops on three hydrophobic surfaces in different vapors are measured. In water-soluble vapors, a substantial decrease is observed in contact angles. This decrease can indeed be explained by a vapor-induced change in the interfacial tensions. The very low contact angle hysteresis on PDMS surfaces in saturated n-hexane and toluene vapor cannot be explained by a change in interfacial tensions. The observation supports the hypothesis that these vapors adsorb into the PDMS and form a lubricating layer. It is hoped that these findings help to solve fundamental problems and contribute to applications, such as anti-icing, heat transfer, and water collection.

1. Introduction

The introduction of Young's equation (**Figure 1**a) started a quantitative treatment of contact angle phenomena. Young's equation predicts the equilibrium contact angle from interfacial surface energies:[1] $\gamma_{LV}\cos\theta = \gamma_{SV} - \gamma_{SL}$. Here, γ_{LV}, γ_{SV}, and γ_{SL} are the liquid–vapor, solid–vapor, and solid–liquid interfacial energies, respectively. It can be derived by a force balance: in equilibrium, the horizontal forces acting on the contact line need to balance. Despite the fact that Young's equation[2] is

widely used, little research has been carried out to analyze the effect of the vapor. Boyd and Livingston[2] in 1942, and later Ward and Wu[3] in 2007 pointed out that the adsorption of vapor to the free solid surface is supposed to change contact angles because of the reduction in γ_{SV}. In 1988, Yekta-Fard and Ponter[4] measured no change in water contact angles of water drops on Teflon when they are exposed to the vapor of cyclohexane, decane, or undecane. Several authors[5] studied the change of the surface tension of water due to the adsorption of organic vapors.

In many natural phenomena and industrial applications, the sliding of drops on surface is important, such as coating,[6] energy conversion,[7] and water harvesting,[8] or for glasses or windscreens in rain. In these cases, one needs to discriminate between advancing θ_a and receding contact angles θ_r. The difference between the two is called contact angle hysteresis. It can be caused by surface heterogeneity, roughness, or adaptation.[9] Contact angle hysteresis is important because it determines the friction force of sessile drops: $F = k\gamma_{LV}w(\cos\theta_r - \cos\theta_a)$.[2,10] Here, $k \approx 1$ is a shape factor and w is the width of the contact area between drop and solid surface.

Despite remarkable developments, the mechanism for drop mobility on surfaces is far from being understood nor controlled. In this respect, surfaces coated with poly(dimethylsiloxane) (PDMS) brushes have attracted great interest because of their low contact angle hysteresis.[11] In a recent paper, we demonstrated that the contact angle hysteresis of water drops on PDMS-coated surfaces is further reduced, when the system is exposed to toluene vapor.[12] We explained the effect by the lubricating action of the vapor being adsorbed in the PDMS layer. This hypothesis was supported by an increase of layer thickness in toluene vapor detected by atomic force microscopy. That polymer brushes adsorb solvent vapors is indeed known.[13]

Khatir and Golovin commented that the same reduction in contact angle hysteresis can be explained simply by a change in γ_{LV}, γ_{SV}, and γ_{SL}.[14] As a result, the force balance at the contact line and the contact angles change. It is indeed known, that when exposing water to the vapor of an organic liquid,

S. Li, H.-J. Butt
Max Planck Institute for Polymer Research
Ackermannweg 10, 55128 Mainz, Germany
E-mail: butt@mpip-mainz.mpg.de

The ORCID identification number(s) for the author(s) of this article can be found under https://doi.org/10.1002/adma.202301905.

ADVANCED
SCIENCE NEWS
www.advancedsciencenews.com
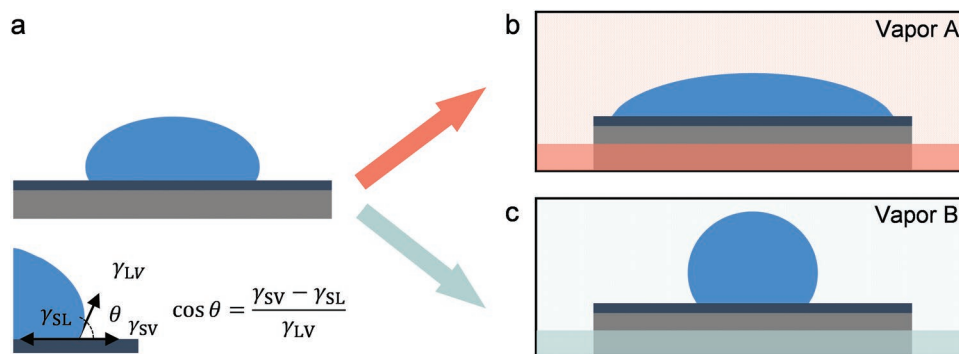
ADVANCED
MATERIALS
www.advmat.de

Figure 1. a) Schematic of a sessile water drop on a solid surface and Young's equation. b,c) Schematically showing a possible change of contact angles after exposing the surface to different vapors.

its surface tension changes due to adsorption and enrichment of the organic molecules.[5,15] That vapor adsorbs to the free solid surface and may decrease γ_{SV} is also known.[2] The comment motivated us to study more in general the effect of organic vapors on contact angles and contact angle hysteresis of water drops on hydrophobic surfaces. We try to answer three questions. How do water contact angles change in different organic vapors (Figure 1b,c)? Can these changes be explained by changes of the interfacial energies? Can a change in γ_{LV}, γ_{SV}, and γ_{SL} explain the low contact angle hysteresis observed on PDMS in n-hexane, cyclohexane, and toluene vapor?

2. Results and Discussion

To answer the questions, we measured the water contact angles on various hydrophobic surfaces in different vapor environments. As representatives, we choose three hydrophobic surfaces (Figure S1, Supporting Information); all surfaces were made as described in the literature.[12,16] 1) PDMS-coated silicon wafers—briefly, PDMS was grafted by immersing the silicon wafer into a solution which contained 40 mL toluene (with saturated water) and 1.4 mL dimethyldichlorosilane. 2) 1H,1H,2H,2H-perfluorodecyltrimethoxysilane (PFDTS)-coated silicon wafers—PFDTS was coated using a chemical vapor deposition method, by putting silicon wafers into a vacuum desiccator (30 mbar) with 20 μL 1H,1H,2H,2H-perfluorodecyltrimethoxysilane added in the bottom for 3 h. 3) Teflon AF (amorphous fluoropolymer) on gold was prepared by dip coating; the sputter-coated gold glass slides were withdrawn from the solution (1 wt% Teflon AF1600 in perfluorotributylamine) at a constant speed of 10 mm min^{-1}. See the Supporting Information for preparation details. To suppress electrostatic effects, all substrates have a high dielectric permittivity or a conductive layer underneath. The root-mean-square surface roughness of all surfaces as measured by atomic force microscopy was less than 1 nm. As vapors, we used n-hexane, cyclohexane (CYC), toluene, dimethylsulfoxide (DMSO), ethanol, and tetrahydrofuran (THF). DMSO, ethanol, and THF are miscible with water. n-Hexane, CYC, and toluene are immiscible and only dissolve to a low concentration in water; the saturation concentrations are 9.5, 55, and 515 ppm, respectively.[17]

To measure water contact angles in vapor environment, we used a goniometer (OCA 35, DataPhysics Instruments) equipped with a custom-made closed metal chamber (Figure S2, Supporting Information), where two glass windows are inserted for visualization. The solvent was inserted at the bottom of the chamber. Inside the chamber, the surface was mounted in a way that it did not get into direct contact with the liquid solvent. The chamber was sealed for more than 10 min before conducting contact angle measurements to generate a stable vapor atmosphere. Videos of sessile drops in side view were recorded when changing water volume gradually (1 μL s^{-1}) between 5 and 20 μL using a motorized Hamilton syringe. Advancing and receding contact angles were determined by fitting an ellipse model to the contour images.

When exposing water drops to vapor of cyclohexane or toluene, the advancing and receding contact angles did not change significantly (**Figure 2**a). In hexane, they increased slightly ($\approx 4°$). When using soluble vapors, the contact angles decreased. The higher the saturation vapor pressure, the more the contact angles decreased (**Table 1**). For example, the advancing contact angles on a PDMS surface in hexane vapor and air were 110° and 106°, respectively, while it was only $\theta_a^v = 87°$ and 73° in ethanol and THF vapor, respectively.

To answer the second and third questions, we measured the surface tension of water in different vapors using the pendent drop method (DSA100E, Krüss).[18] To generate a saturated vapor environment, the liquid was inserted at the bottom of a custom-made closed metal chamber (Figure S2, Supporting Information). After waiting 10 min to reach saturation, a hanging water drop was introduced and imaged in side view. Real-time results were obtained every second by fitting the drop shape with the Laplace equation with the density of water using a built-in program. We report the water's surface tension 2 min after placing the drop into the chamber (Table 1). 2 min is the same time delay as used for contact angle measurements.

The surface tensions of water drops in ethanol, THF, and DMSO vapors vapor decreased to 37, 36, and 58 mN m^{-1}, respectively. These values are lower than the ones in n-hexane, cyclohexane, and toluene vapors, which were 67, 69, and 63 mN m^{-1}, respectively. The low effect in DMSO vapor is attributed to the low saturation vapor pressure of DMSO.

To answer the second question, we first analyze which effect a change of γ_{LV} has, by keeping all other interfacial energies constant. Which contact angle is expected, if γ_{LV} changes from the value in air to the one measured in vapor while keeping γ_{SV} and γ_{SL} constant? To answer this question,
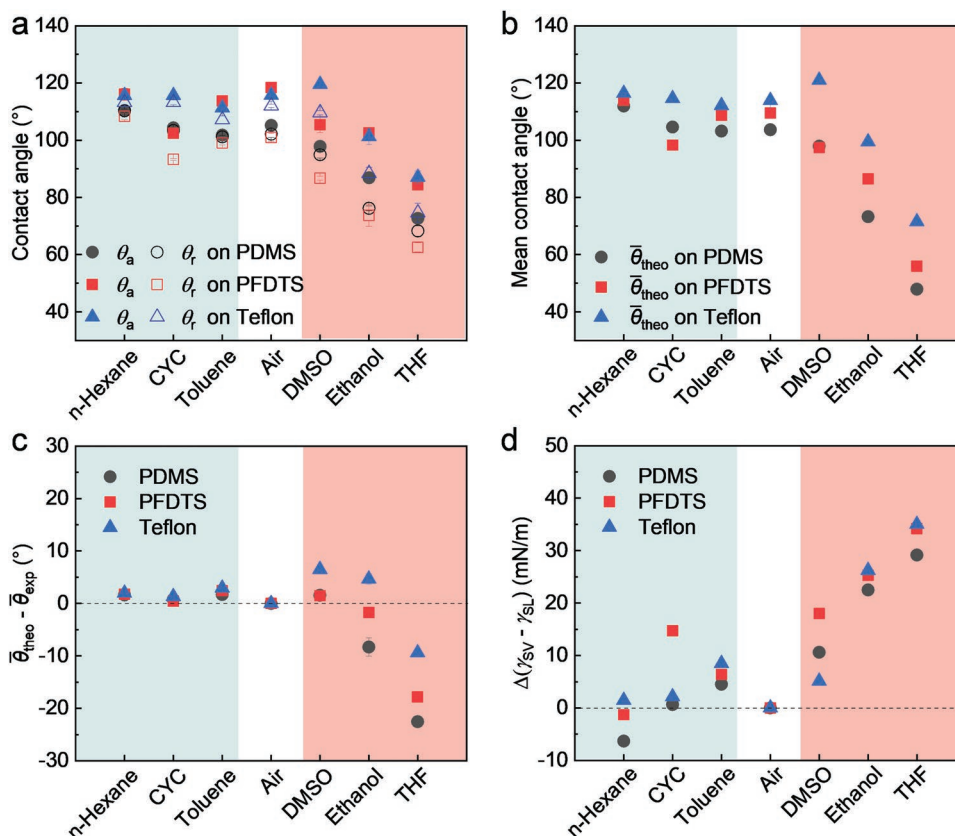
Figure 2. Contact angles of water on PDMS-coated surfaces, PFDTS-coated surfaces, and Teflon films in different vapors: n-hexane, CYC, toluene, air, DMSO, ethanol, and THF. a) Experimental advancing θ_a and receding θ_r contact angles. b) Theoretical mean contact angles calculated with $\cos\overline{\theta}_{theo} = \frac{72\,mN\,m^{-1}}{\gamma_{LV}^v}\cos\overline{\theta}^{air}$. Here, γ_{LV}^v is the surface tension of water in the respective vapor and on the respective surface. $\overline{\theta}^{air}$ is the measured mean contact angle in air of the same surface. c) Difference of expected contact angle (assuming $\gamma_{SV}^v - \gamma_{SL}^v = \gamma_{SV}^{air} - \gamma_{SL}^{air}$) and the experimental value in the respective vapor and on the respective surface, $\overline{\theta}_{theo} - \overline{\theta}_{exp}$. d) Change of $\gamma_{SV} - \gamma_{SL}$ in different vapor environments and in air. Green and red shadows denote results in water-soluble vapor and water-insoluble vapor, respectively.

we compare the experimental mean contact angles (Figure S3, Supporting Information) with contact angles predicted by Young's equation. "Mean" contact angles refer to the mean of the cosines: $\cos\overline{\theta} = (\cos\theta_a + \cos\theta_r)/2$. In a strict sense, Young's equation is only valid in equilibrium. Thus, we assume that the mean contact angle is an approximation for the equilibrium value. Applying Young's equation to the mean contact angle in a vapor leads to $\cos\overline{\theta} = (\gamma_{SV}^v - \gamma_{SL}^v)/\gamma_{LV}^v$, where the superscript

"v" indicates "vapor." Assuming that $\gamma_{SV}^v - \gamma_{SL}^v = \gamma_{SV}^{air} - \gamma_{SL}^{air}$, having measured γ_{LV}^v, and with Young's equation applied to the mean experimental contact in air, $\overline{\theta}^{air}$, we obtain an expected mean contact angle $\cos\overline{\theta}_{theo} = \frac{72\,mN\,m^{-1}}{\gamma_{LV}^v}\cos\overline{\theta}^{air}$.

The expected mean contact angles (Figure 2b) agree with measured contact angles (Figure 2a and Figure S3 (Supporting Information)) for n-hexane, cyclohexane, and toluene within the error of our measurements. This agreement is not surprising, considering that the contact angles were not much affected by the vapor. Substantial deviations were, however, observed for the soluble vapors ethanol and THF. Plotting the difference between the expected and measured contact angles (Figure 2c) shows that the measured contact angles tended to be lower than the expected contact angles. In particular, in THF vapor, the measured contact angles were 10°–23° lower than the calculated ones. Thus, a change from $\gamma_{LV}^v = 72\,mN\,m^{-1}$ to the value measured in vapor γ_{LV}^v cannot explain the observed changes in mean contact angles for soluble vapors. We conclude that for soluble vapors the solid–vapor and/or the solid–liquid interfacial energies change upon exposition to the vapor.

To be able to describe the changes in mean contact angles, we need to take into account a change of $\gamma_{SV} - \gamma_{SL}$. In particular,

Table 1. Liquid and vapor properties at room temperature (23 ± 2 °C).[19]

	Saturated vapor pressure [kPa]	γ_{LV} of pure liquid [mN m^{-1}]	γ_{LV} in the vapor after 2 min [mN m^{-1}]	Hansen solubility parameters [cal$^{1/2}$ cm$^{-3/2}$]
Water	3.17	72	72 ± 1	23
n-Hexane	20.4	18	67 ± 1	7
Cyclohexane	13.0	26	69 ± 1	8
Toluene	3.79	28	63 ± 1	9
DMSO	0.08	43	58 ± 2	13
Ethanol	7.91	22	37 ± 4	13
THF	21.6	26	36 ± 1	10

the water-soluble vapors indicate that we need to consider a change of the interfacial energy γ_{SL} due to the enrichment of DMSO, ethanol, or THF at the solid–liquid interface. How big does this difference between $\gamma_{SV} - \gamma_{SL}$ in air and vapor need to be to account for the observed change in contact angles? To estimate this difference, we calculate

$$\Delta(\gamma_{SV} - \gamma_{SL}) \equiv (\gamma_{SV}^{v} - \gamma_{SL}^{v}) - (\gamma_{SV}^{air} - \gamma_{SL}^{air})$$
$$= \gamma_{LV}^{v} \cos\overline{\theta}^{v} - 72\,\text{mN m}^{-1} \cdot \cos\overline{\theta}^{air} \qquad (1)$$

where $\overline{\theta}^{v}$ is the experimental mean contact angle in a specific vapor. On the left side of Equation (1), all parameters were determined experimentally. As shown in Figure 2d, $\Delta(\gamma_{SV} - \gamma_{SL})$ in all vapors is positive (except n-hexane). Specifically, in ethanol and THF, the value of $\Delta(\gamma_{SV} - \gamma_{SL})$ reaches more than 20 mN m^{-1}. It is highly unlikely that $\gamma_{SV}^{v} > \gamma_{SV}^{air}$, because a spontaneous adsorption of vapor to the solid surface should decrease the solid–vapor interfacial energy.[2,3] For this reason, we believe that this increase in $\Delta(\gamma_{SV} - \gamma_{SL})$ is mainly caused by an adsorption of dissolved vapor molecules to the solid–liquid interface, resulting in a decrease of γ_{SL}.

To answer the third question, we investigate contact angle hysteresis in air $\Delta\theta^{air} = \theta_{a}^{air} - \theta_{r}^{air}$ and vapor $\Delta\theta^{v} = \theta_{a}^{v} - \theta_{r}^{v}$. Here, θ_{a}^{air} and θ_{r}^{air} are the measured advancing and receding contact angles in air. θ_{a}^{v} and θ_{r}^{v} are the respective contact angles in vapor. Contact angle hysteresis depends on the vapor (**Figure 3**a and Table S1 (Supporting Information)). For the water-soluble vapors, $\Delta\theta^{v}$ showed a trend to be higher than in air. For the nonsoluble vapors, the measured contact angle hysteresis $\Delta\theta^{v}$ tended to be lower than in air. In particular, on the PDMS surfaces, much lower contact angle hysteresis was observed than in air.

In an attempt to explain the changing contact angle hysteresis by changing interfacial energies, we apply Young's equation locally. We assume that the interfacial energies close to the contact line need to be inserted into Young's equation and that the interfacial energies are different for the advancing and receding sides. The assumption of local validity of Young's equation is supported by the fact that just before the drop starts to slide, the forces acting on the contact line on the front and rear side are balanced. With this assumption, we estimate the "expected" advancing and receding contact angles in the vapor phase $\theta_{a,\,theo}^{v}$ and $\theta_{r,\,theo}^{v}$ from the respective advancing and receding contact angles measured in air, θ_{a}^{air} and θ_{r}^{air}, by

$$\cos\theta_{a,\,theo}^{v} = \frac{\gamma_{L}^{air}\cos\theta_{a}^{air} + \Delta(\gamma_{SV} - \gamma_{SL})}{\gamma_{LV}^{v}} \qquad (2)$$

$$\cos\theta_{r,\,theo}^{v} = \frac{\gamma_{L}^{air}\cos\theta_{r}^{air} + \Delta(\gamma_{SV} - \gamma_{SL})}{\gamma_{LV}^{v}} \qquad (3)$$

To derive these equations, we reason that at the advancing side

$$\cos\theta_{a,\,theo}^{v} = \frac{\gamma_{SV}^{v} - \gamma_{SL}^{v}}{\gamma_{LV}^{v}}$$
$$= \frac{(\gamma_{SV}^{air} - \gamma_{SL}^{air}) + \Delta(\gamma_{SV} - \gamma_{SL})}{\gamma_{LV}^{v}}$$
$$= \frac{\gamma_{L}^{air}\cos\theta_{a}^{air} + \Delta(\gamma_{SV} - \gamma_{SL})}{\gamma_{LV}^{v}} \qquad (4)$$
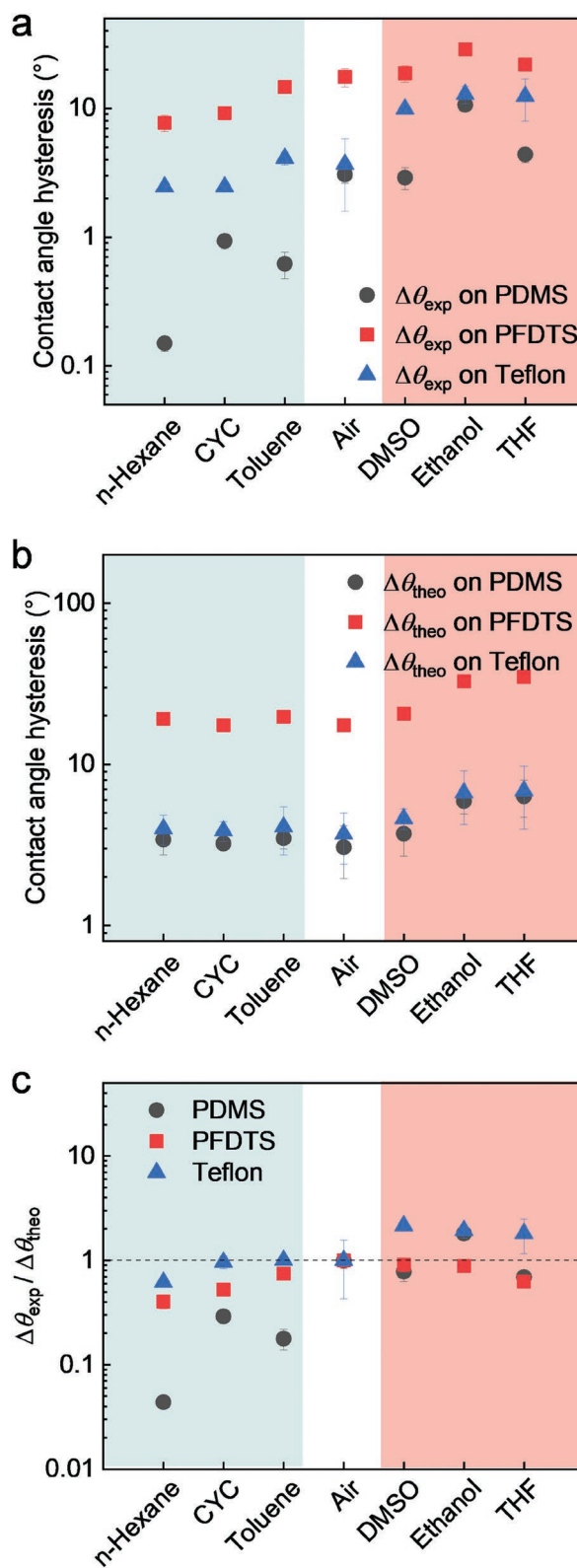

Figure 3. Contact angle hysteresis obtained on PDMS-coated surfaces, PFDTS-coated surfaces, and Teflon films. a) Experimental contact angle hysteresis $\Delta\theta_{exp}$. b) Theoretical contact angle hysteresis $\Delta\theta_{theo}$ calculated with Equations (2) and (3). c) Ratio of experimental contact angle hysteresis to theoretical values $\Delta\theta_{exp}/\Delta\theta_{theo}$. Green and red shadows denote results in water-soluble vapor and water-insoluble vapor, respectively.

Here, the interfacial energies in the first two equations refer to the ones close to the advancing contact line. We can write a similar equation for the receding side, assuming that to derive Equation (3), the interfacial energies close to the receding contact line need to be considered.

With Equations (2) and (3), we calculate the expected contact angle hysteresis in vapor (Figure 3b) and compared it to experimental results (Figure 3c). Experimental values for the contact angle hysteresis deviated substantially from the calculated values (Table S2 in the Supporting Information for details). For the water-insoluble vapors, the contact angle hysteresis tends to be lower than theoretical values. In particular, for the PDMS surfaces, the observed contact angle hysteresis was 71–96% lower than the theoretical ones. We attribute these low $\Delta\theta_{exp}$ values to the lubricating effect of the vapor. Vapor is absorbed in the PDMS and lubricates the motion of the contact line.[20] We conclude, that the change of interfacial energies cannot explain the change of contact angle hysteresis. Physisorption into the PDMS plays an important role. This hypothesis is supported by the correlation of $\Delta\theta_{exp}$ with the difference of Hansen solubility parameters[19,21] between the vapor and the PDMS coating ($\Delta\delta = \delta_V - \delta_{PDMS}$). Originally developed to decide if a substance is soluble in another, it has also been successfully applied to indicate the uptake of solvents by PDMS.[21] The lower the difference between Hansen parameters, the more vapor adsorbs in the PDMS brush and the lower the contact angle hysteresis become.

3. Conclusion

Water advancing and receding contact angles do not change significantly for vapors, which are immiscible with water. By contrast, for soluble vapors, we detected a substantial decrease of contact angles. This decrease can be explained by an adsorption of dissolved molecules to the solid–liquid interfaces and the resulting reduction of γ_{SV}. Thus, in accordance with Khatir and Golovin, a change in the mean contact angle can be explained by vapor-induced changes in the interfacial energies. However, the observed decrease in contact angle hysteresis on PDMS cannot be explained by changes in γ_{LV}, γ_{SL}, and γ_{SV}. We attribute them to an uptake of vapor by the PDMS and the formation of a lubricating layer. Our findings are directly relevant to situations where droplets occur such as water collection, heat transfer, and power generation applications. The insight that background vapor influences drop contact angles may open new avenues for drop manipulation.

Supporting Information

Supporting Information is available from the Wiley Online Library or from the author.

Acknowledgements

Conflict of Interest

The authors declare no conflict of interest.

Keywords

[1] a) T. Young, *Philos. Trans. R. Soc. London* **1805**, *95*, 65; b) P. S. Laplace, Traité de mécanique céleste/par PS Laplace...; tome premier [-quatrieme], de l'Imprimerie de Crapelet, Paris, France **1805**.

[2] a) G. Boyd, H. Livingston, *J. Am. Chem. Soc.* **1942**, *64*, 2383; b) R. J. Good, *J. Am. Chem. Soc.* **1952**, *74*, 5041; c) R. Shuttleworth, G. Bailey, *Discuss. Faraday Soc.* **1948**, *3*, 16; d) C. Huh, S. Mason, *J. Colloid Interface Sci.* **1977**, *60*, 11; e) J. Joanny, P.-G. de Gennes, *J. Chem. Phys.* **1984**, *81*, 552; f) P.-G. de Gennes, P. Brochard, D. Quéré, *Capillarity and Wetting Phenomena: Drops, Bubbles, Pearls, Waves*, Springer, New York **2004**; g) C. Furmidge, *J. Colloid Sci.* **1962**, *17*, 309.

[3] C. A. Ward, J. Wu, *J. Phys. Chem. B* **2007**, *111*, 3685.

[4] M. Yekta-Fard, A. B. Ponter, *J. Colloid Interface Sci.* **1988**, *126*, 134.

[5] a) H. Kamusewitz, W. Possart, D. Paul, *Int. J. Adhes. Adhes.* **1993**, *13*, 243; b) V. B. Fainerman, E. V. Aksenenko, V. I. Kovalchuk, R. Miller, *Colloids Surf., A* **2016**, *505*, 118; c) T. Kairaliyeva, V. B. Fainerman, E. V. Aksenenko, V. I. Kovalchuk, Y. I. Tarasevich, R. Miller, *Colloids Surf., A* **2017**, *532*, 541; d) N. Mucic, N. Moradi, A. Javadi, E. V. Aksenenko, V. B. Fainerman, R. Miller, *Colloids Surf., A* **2015**, *480*, 79.

[6] H.-J. Streitberger, A. Goldschmidt, *BASF Handbook Basics of Coating Technology*, European Coatings, Munster, Germany **2018**.

[7] W. Xu, H. Zheng, Y. Liu, X. Zhou, C. Zhang, Y. Song, X. Deng, M. Leung, Z. Yang, R. X. Xu, Z. L. Wang, X. C. Zeng, Z. Wang, *Nature* **2020**, *578*, 392.

[8] Y. Zheng, H. Bai, Z. Huang, X. Tian, F. Q. Nie, Y. Zhao, J. Zhai, L. Jiang, *Nature* **2010**, *463*, 640.

[9] a) H.-J. Butt, J. Liu, K. Koynov, B. Straub, C. Hinduja, I. Roismann, R. Berger, X. Li, D. Vollmer, M. Steffen, M. Kappl, *Curr. Opin. Colloid Interface Sci.* **2022**, *59*, 101574; b) H.-J. Butt, R. Berger, W. Steffen, D. Vollmer, S. A. L. Weber, *Langmuir* **2018**, *34*, 11292.

[10] a) Y. I. Frenkel, J. Exp. Theor. Phys. (USSR), 18, 659, 1948; translation by V. Berejnov: arXiv: physics/0503051, **2005**; b) A. Buzágh, E. Wolfram, *Kolloid-Z.* **1958**, *157*, 50.

[11] a) X. Zhao, M. A. R. Khandoker, K. Golovin, *ACS Appl. Mater. Interfaces* **2020**, *12*, 15748; b) L. Wang, T. J. McCarthy, *Angew. Chem., Int. Ed.* **2016**, *55*, 244.

[12] S. Li, Y. Hou, M. Kappl, W. Steffen, J. Liu, H. J. Butt, *Adv. Mater.* **2022**, *34*, 2203242.

[13] G. C. Ritsema van Eck, E. M. Kiens, L. B. Veldscholte, M. Brió Pérez, S. de Beer, *Langmuir* **2022**, *38*, 13763.

[14] B. Khatir, K. Golovin, *Adv. Mater.* **2023**, https://doi.org/10.1002/adma.202208783.

**ADVANCED
SCIENCE NEWS**

www.advancedsciencenews.com

**ADVANCED
MATERIALS**

www.advmat.de

[15] a) B. A. Pethica, M. L. Glasser, *Langmuir* **2005**, *21*, 944; b) O.-S. Kwon, H. Jing, K. Shin, X. Wang, S. K. Satija, *Langmuir* **2007**, *23*, 12249; c) A. Javadi, N. Moradi, H. Möhwald, R. Miller, *Soft Matter* **2010**, *6*, 4710.

[16] X. Li, P. Bista, A. Z. Stetten, H. Bonart, M. T. Schür, S. Hardt, F. Bodziony, H. Marschall, A. Saal, X. Deng, R. Berger, S. A. L. Weber, H.-J. Butt, *Nat. Phys.* **2022**, *18*, 713.

[17] a) Y. Yang, D. J. Miller, S. B. Hawthorne, *J. Chem. Eng. Data* **1997**, *42*, 908; b) K. Verschueren, *Handbook of Environmental Data on Organic Chemicals*, Vol. *1*, John Wiley and Sons, Inc., New York **2001**; c) S. Poulson, R. Harrington, J. Drever, *Talanta* **1999**, *48*, 633; d) C. McAuliffe, *J. Phys. Chem.* **1966**, *70*, 1267.

[18] a) J. D. Berry, M. J. Neeson, R. R. Dagastine, D. Y. C. Chan, R. F. Tabor, *J. Colloid Interface Sci.* **2015**, *454*, 226; b) C. E. Stauffer, *J. Phys. Chem.* **1965**, *69*, 1933.

[19] a) T. E. Daubert, R. P. Danner, *Physical and Thermodynamic Properties of Pure Chemicals: Data Compilation*, Taylor & Francis, Washington, DC, USA **1989**; b) G. I. Mantanis, R. A. Young, *Wood Sci. Technol.* **1997**, *31*, 339; c) D. R. Lide, *CRC Handbook of Chemistry and Physics*, CRC Press, Boca Raton, FL, USA **2004**; d) C. M. Hansen, *Hansen Solubility Parameters: A User's Handbook*, CRC Press, Boca Raton, FL, USA **2007**.

[20] a) H. Liu, P. Zhang, M. Liu, S. Wang, L. Jiang, *Adv. Mater.* **2013**, *25*, 4477; b) A. Eifert, D. Paulssen, S. N. Varanakkottu, T. Baier, S. Hardt, *Adv. Mater. Interfaces* **2014**, *1*, 1300138; c) D. Daniel, J. V. I. Timonen, R. Li, S. J. Velling, M. J. Kreder, A. Tetreault, J. Aizenberg, *Phys. Rev. Lett.* **2018**, *120*, 244503.

[21] a) P. Sukitpaneenit, T.-S. Chung, in *Hollow Fiber Membranes*, Elsevier, Amsterdam, The Netherlands **2021**; b) Q. Su, J. Zhang, L.-Z. Zhang, *Desalination* **2020**, *476*, 114246; c) W. Zhang, Y. Zhang, C. Lu, Y. Deng, *J. Mater. Chem.* **2012**, *22*, 11642; d) F. Machui, S. Langner, X. Zhu, S. Abbott, C. J. Brabec, *Sol. Energy Mater. Sol. Cells* **2012**, *100*, 138; e) J. N. Lee, C. Park, G. M. Whitesides, *Anal. Chem.* **2003**, *75*, 6544; f) R. L. Scott, *J. Am. Chem. Soc.* **1948**, *70*, 4090.

2301905 (6 of 6)